Applied Energy 416 (2026) 127983

Contents lists available at ScienceDirect

Applied Energy

journal homepage: www.elsevier.com/locate/apen

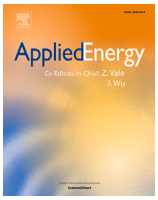

Consumer safety-oriented scheduling of rotating power outages during heat waves

Luis Rodriguez-Garcia*, Miguel Heleno, Wanni Zhang, Han Li, Kaiyu Sun, Tianzhen Hong

Lawrence Berkeley National Laboratory, Berkeley, CA, USA

HIGHLIGHTS

- Customer vulnerability quantified via outage-induced overheating risk metric.
- Distribution feeders prioritized for rotating outages based on overheating sensitivity to power outages.
- Outage sequence and duration assigned to meet a utility load reduction target while minimizing potential overheating risk.
- Strategy evaluated using real power distribution data and high-fidelity building energy simulations.
- Proposed approach reduces overheating risk compared to random and uninformed outage schedules.

ARTICLE INFO

Keywords:
Rotating outages
Overheating risk
Heat wave
Building thermal simulation
Distribution systems

ABSTRACT

Extreme heat events have widespread effects on power systems, reducing available generation capacity, limiting transmission capabilities, and causing unusual demand patterns on the consumer side. As these combined effects expose bulk transmission systems to potential large-scale blackouts, utilities may be required to schedule and apply rotating outages, by temporarily and alternately disconnecting distribution substations to reduce overload. However, utilities lack mechanisms to inform these events, exacerbating the negative effects of heat waves on affected communities. This paper introduces a novel framework for scheduling rotating outages during heat waves while considering impacts on consumers' safety. Instead of random sequential load shedding, we propose a methodology to rotate power outages considering a metric that quantifies the indoor overheating risk of groups of consumers during a power outage. The overheating risk is derived from a detailed building simulation using CityBES, where the buildings are modeled based on available data—use type, year built, floor area, number of stories, location—while presence of air conditioning and occupancy are calibrated from smart meter data. Based on the metric, an algorithm to schedule the rotating outages is applied to prioritize feeders for disconnection at each hour according to their overheating risk to meet a utility load reduction target. Applied to two substations and seven feeders in the Portland General Electric territory, the results show that this approach effectively leads to the lowest overheating risk during the resulting outage schedules, with an average 10.1% lower overheating compared to uninformed schedules.

1. Introduction

1.1. Motivation

The Western United States has been historically impacted by heat-related events. Particularly, heat waves—defined as an extended periods of abnormally high temperatures in a given area—led to 21,518 heat-related deaths in the US from 1999 to 2003, with the largest record of 2323 in 2023 [1]. In addition to the impact on public health and the increased risk of heat-related illnesses, excessive heat events also negatively influence the operation of both transmission and distribution power grids.

Traditionally, electricity is delivered to end-use consumers through a structure comprising generation, transmission, and distribution, as shown in Fig. 1. At the generation stage, power plants transform energy from primary energy resources—e.g., water, wind, solar, fossil fuels—into electricity. This energy is transported over long distances through the high-voltage transmission networks to major load centers.

* Corresponding author.
Email address: luisrodriguezgarcia@lbl.gov (L. Rodriguez-Garcia).

https://doi.org/10.1016/j.apenergy.2026.127983
Received 15 September 2025; Received in revised form 18 December 2025; Accepted 22 April 2026
Available online 4 May 2026

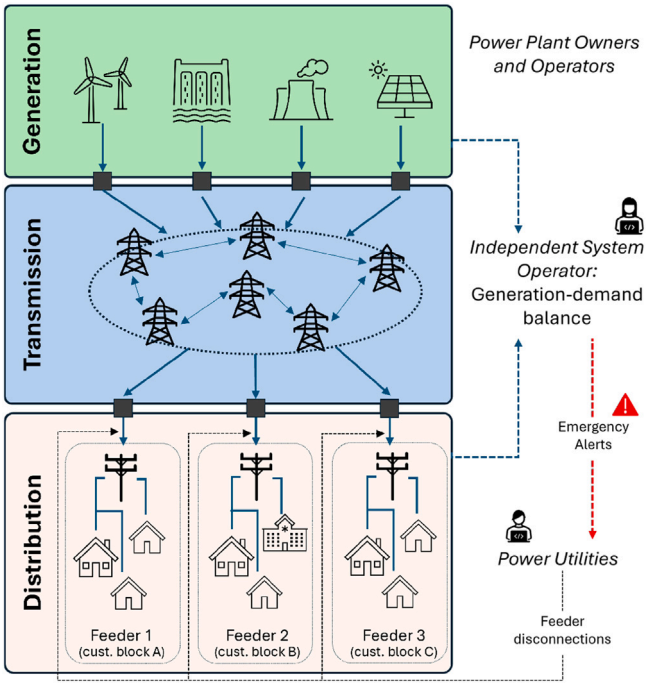

Fig. 1. Power generation, transmission, and distribution process: the role of independent system operators and power utilities in rotating outages.

From there, distribution grids deliver this electricity at lower voltages to residential, commercial, and industrial consumers.

The reliable operation of this complex infrastructure depends on maintaining the balance between electricity supply and demand. In many regions, Independent System Operators (ISOs) are responsible for coordinating this balance, to avoid instability and potential large-scale blackouts. ISOs schedule and dispatch generation resources, monitor grid conditions in real time, and communicate operational requirements to both power plant operators and power utilities.

The power system operation becomes challenging in a heat wave scenario. Customers on the distribution grids increase their electricity consumption from air conditioning (AC) operation to mitigate the impact of heat. Excessive heat can also impair the operation of transmission systems by reducing the generation capacity of power plants [2], and lowering the transmission system's ability to transfer power from generation sources to the demand locations [3]. If a potential large-scale blackout risk due to increased demand and reduced generation is identified, ISOs encourage power utilities to implement strategies aimed at reducing energy consumption among customers in their territory.

For instance, the California Independent System Operator (CAISO) issues two levels of Energy Emergency Alerts to initially encourage and then urge consumers to conserve energy and help preserve grid reliability [4]. If these measures fail to maintain the demand under a certain level, a third-level emergency alert is triggered, where ISOs instruct utilities to prepare for—and potentially implement—rotating outages to reduce load by curtailing electricity to customers. Recently, an extreme heat wave affected the Western US in August 2020. As the load during this heat wave period was underestimated, CAISO ordered the disconnection of two blocks of 500 MW and one block of 500 MW, respectively, on August 14th and August 15th. This led to the de-energization of 491,600 customers on August 14th, and 321,000 customers on August 15th [5]. The number of emergency alerts and the duration of interruption per quarter for WECC interconnection is shown in Fig. 2(a) and (b), respectively, from 2018 (Q4) to 2022 (Q3). It is worth noting from Fig. 2(a) that the number of these emergency alerts spikes during Q3 for 2020 and 2022, corresponding to years where heat wave events were registered. Similarly from Fig. 2(b), the duration of interruptions reaches more than 200 minutes during these periods.

During rotating outages, utilities temporarily disconnect groups of customers by alternately de-energizing feeders at selected substations to meet the ISO requirement. While load curtailment is undesirable, this controlled de-energization lowers the risk of widespread blackouts and massive customer disconnections. Utilities will normally exclude feeders with critical facilities—such as hospitals—from their rotating outage schedules, while the rest of the feeders are prioritized based on pre-identified customer blocks [7] or alphabetical criteria [8]. Therefore, how utilities make these decisions has a critical impact on the affected groups of consumers, as consumers under a rotating outage cannot use their AC compromising their ability to withstand extreme heat.

1.2. Literature review

Rotating outages are undesirable in distribution system operation but their application has helped to mitigate distribution feeder issues, such as the risk of wildfires caused by faults on the grid [9]. However, the effect of concurrent heat waves and power outages on communities has been identified as a matter of concern in recent literature. The impact of the rotating outages during heat waves has been considered as one of elements that influence the technological, social, and policy dimensions of thermal resilience as discussed in existing literature [10]. Simulations of the effect of heat during power outages and passive strategies for its mitigation have been studied for different regions, such as Arizona [11], and California [12]. An assessment of thermal resilience for facilities after power outages during heat waves and cold snaps is presented in

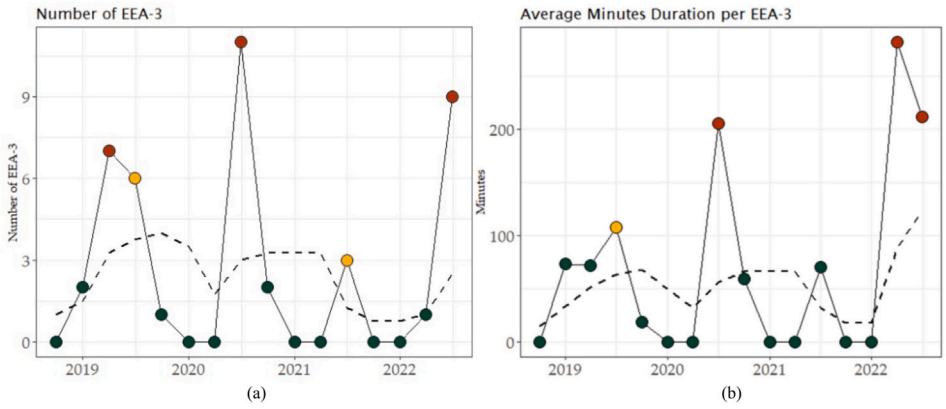

Fig. 2. Emergency alerts in WECC territory from 2018 (Q4) to 2022 (Q3): (a) number of emergency alerts, and (b) duration in minutes [6].

[13]. The effect of outages in communities exposed to extreme heat is discussed on [12], alongside passive strategies that help reduce the related indoor overheating risk, such as natural ventilation, interior blinds, or roof and ceiling insulation.

However, despite the impacts of the power outages during extreme heat events, existing approaches to enhance distribution system resilience through rotating outages have not considered the impact of other external variables to guide the decision-making process. A framework to assess how automation can improve distribution system resilience to extreme temperature events is developed in [14], which aims at ensuring customers' health and safety during extremes, significantly reducing exposure to cold by 93% considering ERCOT data during Winter Storm Uri. A rotating outage scheme based on Advanced Metering Infrastructure (AMI) combined with an outage management system is formulated in [15], where customers selected for rotating outage are chosen based on undiversified demand from AMI data. An optimization-based approach for scheduling fair blackout rotation for distribution systems under extreme weather-induced power outages is presented in [16]. The model defines the logical operation of switches, and optimizes deviations of isolation duration and frequencies between sections. Communication and controllability from distribution automation and grid-edge smart meters to shed loads in a strategic fashion are explored in [17]; however, the approach does not consider attributes related to the customers' safety.

Alternatively to rotating outages that cause discomfort to large portions of consumers affected by the disconnection, brownouts offer a way to reduce grid demand without fully disrupting the distribution grid operation. Five algorithms are developed in [18] to implement a brownout mechanism to distribute loading thresholds among individual consumers in a neighborhood. An integer linear programming model for brownout is formulated in [19], with a modified power adjustment approach to efficiently implement this strategy in real-time. On the other hand, a centralized brownout scheme based on price is formulated for microgrids in [20], based on consumers' priorities for uninterrupted power. The implementation of brownout schemes, however, can be challenging when proper automation at consumers' locations is limited to ensure their proper operation. In addition, vulnerability to extreme weather is not considered.

While existing literature does not incorporate heat vulnerability information into the rotating outage scheduling, some steps include a data-driven approach to plan for rotating power outages as formulated in [21], which infers thermal characteristics from smart thermostat data, and then uses this data to simulate the building thermal resilience during a heat wave; a planning framework for DER siting based on a metric that determines the sensitivity of distribution sections to a power outage is formulated in [22]; and a metric is introduced in [23] to rank nodes with higher vulnerability in terms of overheating, and guide utilities to take actions towards impact mitigation.

1.3. Contributions and paper structure

Current rotating outage protocols do not account for the effect of indoor overheating risk to prioritize actions when necessary. When heat-related effects on customers are neglected, utility actions to protect the grid stability may inadvertently worsen public health outcomes. For this purpose, this paper formulates a methodology to schedule rotating outages based on estimations of indoor overheating risk to be experienced in buildings during power outages. The contributions of this paper are:

- We formulate a metric to prioritize feeders for disconnection during rotating outages, from safest to most sensitive.
- We define a strategy to inform power utilities on how to determine the feeders to be switched at every hour to meet a utility load reduction target while reducing overheating risk.
- We assess the performance of our method in a realistic setup considering building modeling and occupancy characterization based on AMI data.
- We evaluate the performance of the proposed approach versus randomly generated scenarios to compare our proposed method with possible allocations made by power system operators.

The remainder of the paper is organized as follows. Section 2 provides an overview of the methodology for scheduling rotating outages based on overheating risk information. The metric to drive the rotating outage scheduling is formulated in Section 3, which also includes the building simulation procedure for its evaluation. The proposed algorithm for rotating outage scheduling is described in detail in Section 4. Section 5 presents the results of the analysis on two Portland General Electric (PGE) substations. Finally, Section 6 summarizes the conclusions and limitations of the paper, and proposes future work.

2. Overview of the proposed method

The proposed methodology to schedule rotating outages for distribution feeders informed by overheating risk data is described in this section. In order to meet a utility load reduction target, the proposed method establishes feeder disconnection schedules at a given substation, which are informed by the aggregated overheating risk experienced among households subjected to the power interruptions. The methodology proposed in this paper is illustrated in Fig. 3.

To define the schedule, feeders are ranked based on their outage-induced overheating risk, which is a metric that quantifies the accumulated overheating risk experienced by the feeder for every hour of additional disconnection from the power supply. The overheating evaluation is achieved via building simulation to estimate the indoor air temperature in each building when subjected to the power outage. These results, combined with the feeder operational constraints, define the rotating outage strategy. In this case, the operational constraints include the minimum time a feeder has to remain connected before a new disconnection, and the maximum time a feeder can remain de-energized after being disconnected.

The methodology is organized as follows. The proposed metric for driving the feeder disconnection rotation is initially introduced. The

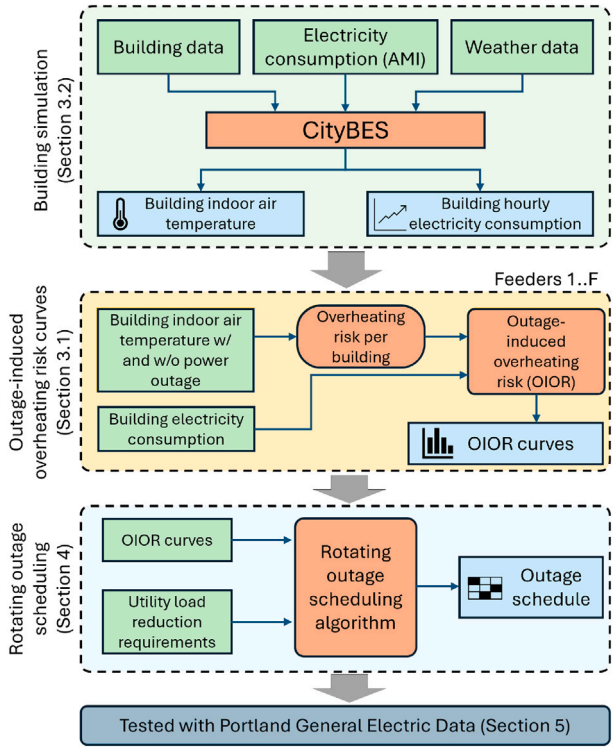

Fig. 3. Methodology for overheating-risk-informed rotating outages scheduling.

evaluation of the metric depends on precisely capturing the indoor air temperature when buildings are exposed to high temperatures during extreme heat. Therefore, a simulation-based approach to estimate indoor temperature is discussed. Using these estimates—with and without power outages—and considering the non-served energy during the rotating outage window, the outage-induced overheating risk is calculated considering different outage durations. Finally, the algorithm to schedule rotating outages based on overheating risk data is formulated.

3. Metric formulation and evaluation

3.1. Overheating sensitivity to power outage

The proposed method for scheduling rotating outages is driven by a metric that relates the aggregated overheating risk in a group of buildings during a power outage to the amount of energy curtailed during such event. More specifically, this metric incorporates the outage-induced overheating risk (OIOR), initially defined in [22] for distribution planning to optimally allocate distributed energy resources, to identify and prioritize feeders where the customers' overheating risk is less sensitive to power outages. OIOR refers to the overheating risk component that is added due to the power outage, i.e., the component of overheating risk that can be avoided through utility action. This action is critical as indoor air temperature in buildings with AC can significantly increase during a power outage, especially under extreme weather conditions such as heatwaves.

To illustrate this formulation for rotating outage scheduling, consider the distribution system of Fig. 4. In this distribution system, a set of B buildings is supplied by a distribution feeder connected to a power substation. The indoor air temperature profiles for some buildings are shown as examples to highlight that each building responds differently to excessive heat and power outages. In some of these cases, both the outage and non-outage induced overheating risks may occur. The sensitivity of overheating risk for a group of customers connected to a feeder that is subject to a power outage is obtained as the ratio between the aggregated OIOR in each of the buildings and the amount of energy to be consumed that—if supplied—would prevent this risk. The OIOR per kWh of energy curtailed for feeder f, for an outage starting at time $\bar{t}$ with a duration d, $\mathcal{O}_{f,\bar{t},d}$, is obtained as,

$$\mathcal{O}_{f,\bar{t},d} = \frac{\sum_{t\in\mathcal{T}}\sum_{b\in\mathcal{B}_f} \max\left\{\theta^O_{b,t} - \max\left\{\theta^N_{b,t}, \theta^T\right\}, 0\right\}\Delta t}{\sum_{t\in\mathcal{T}_d}\sum_{b\in\mathcal{B}_f} p^N_{b,t}\Delta t}, \tag{1}$$

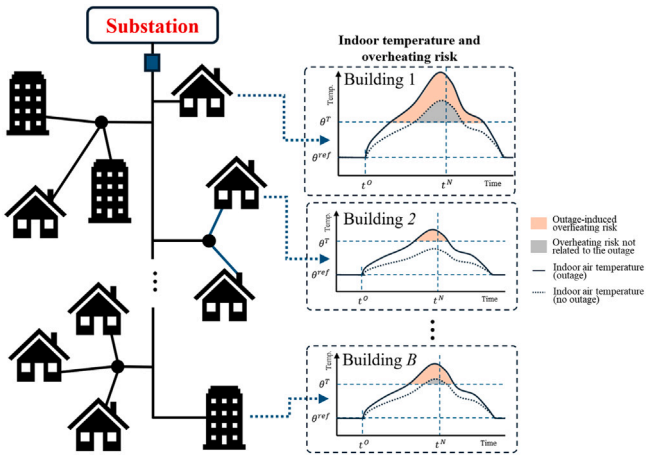

Fig. 4. Effect of the feeder power outage on the overheating risk experienced in buildings supplied by the affected feeder.

where $\theta^O_{b,t}, \theta^N_{b,t}$ are the indoor air temperatures in building b, at time t with and without power outage, respectively, θ^T is the temperature risk threshold, $p^N_{b,t}$ is the power consumed by building b, at time t during the no-outage condition, Δt is the time step between samples related to the time data resolution, $\mathcal{T} = \{\bar{t}, \ldots, \bar{t} + h\}$ is the set of time steps in the overheating risk calculation evaluation window, $\mathcal{T}_d = \{\bar{t}, \ldots, \bar{t} + d\}$ is the set of time steps in the outage window, $\mathcal{B}_f$ is the subset of buildings connected to feeder f. Feeders $f \in \mathcal{F}$ with lower metric values are ranked higher and preferred for disconnection during the heatwave event, if required.

3.2. Building simulation

The building simulation is achieved using CityBES, which is a web-based data and computing platform, focusing on energy modeling and analysis of a city's building stock to support district or city-scale building energy efficiency programs [24].

CityBES employs EnergyPlus, a U.S. Department of Energy flagship physics-based building performance modeling engine, to simulate building energy demand and thermal performance, e.g., indoor air temperature and humidity, for assessing costs and benefits of building retrofits. CityBES integrates open city datasets, e.g., building footprint polygons, tax assessor records, among others, to create a dataset of building stock with characteristics of individual buildings depending on the level of available data. Most buildings have high-level information such as use type, year built, floor area, number of stories, and location. Detailed building information such as construction materials, HVAC system type, lighting and plug loads, as well as operation settings and schedules, is inferred from local building energy codes and standards, representative local building stock surveys, and construction industry practices. The building models can be further calibrated with the AMI data provided by the local utility company in a heuristic approach, aiming to improve the load prediction accuracy of the models during the extreme heat periods.

To obtain the OIOR, the indoor conditions and electricity use are initially simulated during the extreme heat period for normal electricity supply. For the power outage scenario, all the electricity load is disconnected during the extreme heat period and indoor air conditions in this scenario are determined. This is done for the purpose of obtaining the indoor air temperature of each of the buildings during a power outage, and does not intend to represent an actual power system maneuver or malfunction. In order to better reflect real-world situations, occupants are assumed to use natural ventilation to cool down the room whenever possible in both power outage and no outage scenarios.

4. Rotating outage scheduling algorithm

The rotating outage algorithm determines the sequence of feeder disconnections within the rotation window $\mathcal{T}^d$ to satisfy the substation load reduction target r_t while reducing the impact of these disconnections on the overheating risk experienced by households. A complete rotation is achieved when every feeder has been disconnected exactly once before any feeder is disconnected again. This condition is included to avoid frequent disconnections of the feeder with the least overheating risk. The binary variable $x_{f,t}$ indicates the connection status of feeder f at time t, e.g., $x_{f,t} = 1$ means connected. Additional constraints include a maximum outage duration $\overline{d_f}$ per feeder and a minimum reconnection time $\underline{c_f}$ before a feeder can be disconnected again. Decisions are taken at intervals of Δt based on available data resolution, with outage-induced overheating risk $\mathcal{O}_{f,t,d}$ pre-calculated for every outage start time and every outage duration in the rotation window $\mathcal{T}^d$.

4.1. Initial hour ($t = \bar{t}$)

The first procedure allows defining the initial batch of feeders to be disconnected. Let us define the set $\mathcal{F}' \subseteq \mathcal{F}$ as the set of feeders that are

eligible for disconnection. Initially, all feeders are eligible for disconnection, and it is assumed that all feeders are connected at the beginning of the rotating outage window. Let $\mathcal{F}^C$ be the set of connected feeders, $\mathcal{F}^D$ be the set of disconnected feeders, and d_f be the disconnection duration of feeder f.

1. **Initialize counters and sets:** $d_f = 0, \forall f \in \mathcal{F}$. $\mathcal{F}^C \leftarrow \mathcal{F}$, $\mathcal{F}^D \leftarrow \emptyset$, $\mathcal{F}' \leftarrow \mathcal{F}$.
2. **Estimate overheating risk:** Determine the OIOR for each feeder for a one-hour disconnection, i.e., $\mathcal{O}_{f,d_f+1}$.
3. **Identify candidate for disconnection:** Identify the connected feeder $f \in \mathcal{F}'$ with the lowest OIOR,

$$\overline{f} = \arg\min_{f \in \mathcal{F}'} \mathcal{O}_{f,d_f+1}, \tag{2}$$

4. **Disconnect candidate feeder:** Schedule disconnection of feeder $\overline{f}$ for time t. For this, set the connection status for feeder $\bar{f}$ for time t and increase the disconnection time for feeder $\bar{f}$ (3), and remove the feeder $\bar{f}$ from the set $\mathcal{F}'$ (4). In addition, update the sets of connected and disconnected feeders,

$$x_{\overline{f},t} = 0, \quad d_{\overline{f}} \leftarrow d_{\overline{f}} + 1, \tag{3}$$

$$\mathcal{F}' \leftarrow \mathcal{F}' \setminus \{\bar{f}\}. \tag{4}$$

5. **Calculate the substation load** after disconnection P_t^{ss} (5), where $P_{f,t}$ is the power consumed by feeder f at time t,

$$P_t^{ss} = \sum_{f \in \mathcal{F}^C} P_{f,t}, \tag{5}$$

6. **Verify utility load reduction target:** Check if the substation load P_t^{ss} is below the utility disconnection requirement, i.e.,

$$P_t^{ss} \leq \left(1 - r_t/100\right) \sum_{f \in \mathcal{F}} P_{f,t}. \tag{6}$$

If the condition is met, terminate the procedure; the scheduling for hour 1 is concluded. Otherwise, go to Step 3.

4.2. Subsequent hours ($t > \bar{t}$)

The evaluation for each subsequent hour considers the OIOR for an additional hour of disconnection, i.e., $d_f + 1$. For this process, the set of locked feeders $\mathcal{F}^L$ is introduced to represent the reconnected feeders that cannot be candidates for new disconnections until their minimum connected time is met.

Preamble: Consider $t = \bar{t}$, and disconnected time d_f, $\mathcal{F}^C$, $\mathcal{F}^D$, and $\mathcal{F}'$ as obtained from process formulated in Section 4.1. Initialize $c_f \leftarrow 0, \forall f \in \mathcal{F}$; $\mathcal{F}^L \leftarrow \emptyset$; $\mathcal{F}^R \leftarrow \emptyset$.

7. **Advance time:** $t \leftarrow t + 1$. If $t > \bar{t} + d$, stop; otherwise, evaluate $\mathcal{O}_{f,d_f+1}$ for each feeder and continue.
8. **Identify feeders to reconnect ($\mathcal{F}^R$):** A feeder is in $\mathcal{F}^R$ if the feeder has been disconnected for more than its maximum off time $\overline{d_f}$, or, if the feeder overheating risk after one hour of additional disconnection exceeds that of any other eligible connected feeder.
9. **Reconnect candidate feeders:** Feeders in $\mathcal{F}^R$ are reconnected for hour t, i.e., $x_{f,t} = 1, \ \forall f \in \mathcal{F}^R$. The disconnection duration is set to zero, $d_f = 0, \ \forall f \in \mathcal{F}^R$.
10. **Update eligibility to re-disconnect:** For all reconnected feeders, increase their reconnected time c_f by one hour. Remove the feeders where $c_f = \underline{c_f}$ from the set of locked feeders $\mathcal{F}^L$. At this point, include the recently reconnected feeders in the set of locked feeders.
11. **Check load target:** Based on the current connected and disconnected feeders, calculate the substation load (5). If the current load meets the load reduction target (6), let $x_{f,t} = 1$ for all connected feeders and go to Step 7. Otherwise, continue.
12. **Select feeder for disconnection:** If $\mathcal{F}' \neq \emptyset$, identify the eligible connected feeder with the lowest OIOR (2), then, do (3)–(4) and go to Step 11. If $\mathcal{F}' = \emptyset$, feeders that were reconnected previously (except those reconnected during time t, $\mathcal{F}^R$) become available for reconnection. In that case, update the set of eligible feeders for disconnection $\mathcal{F}' \leftarrow \mathcal{F} \setminus \mathcal{F}^L$ and go to Step 11.

5. Results and discussion

5.1. Data and building calibration results

The methodology is applied to data provided by PGE considering two substations and a total of seven feeders. Due to the sensitive nature of the data, the original names of substations and feeders are removed, and replaced by Substation A with 4 feeders and Substation B with 3 feeders. Fig. 5 visualizes the buildings served by each feeder and their distribution in the territory. For the simulation, a total number of 8512 buildings are modeled in CityBES, where their distribution across substations and feeders is summarized in Table 1.

A dataset for buildings covered by each substation was curated with residential buildings dominating the neighborhood. The building characteristics were mainly extracted from PortlandMaps Open Data [25], including building footprint, building type, number of stories, building height, and year built. Assumptions on HVAC were adopted from the 2022 Northwest Energy Efficiency Alliance (NEEA) Residential Building Stock Assessment [26], with 75% of the neighborhood buildings equipped with air conditioning systems. AMI data for the two substations was provided by PGE for the years 2021 and 2023. Local weather data for 2021 was obtained from NASA Prediction Of Worldwide Energy Resources (POWER) for the Portland neighborhood [27]. The highest outdoor temperature occurred on June 28, so

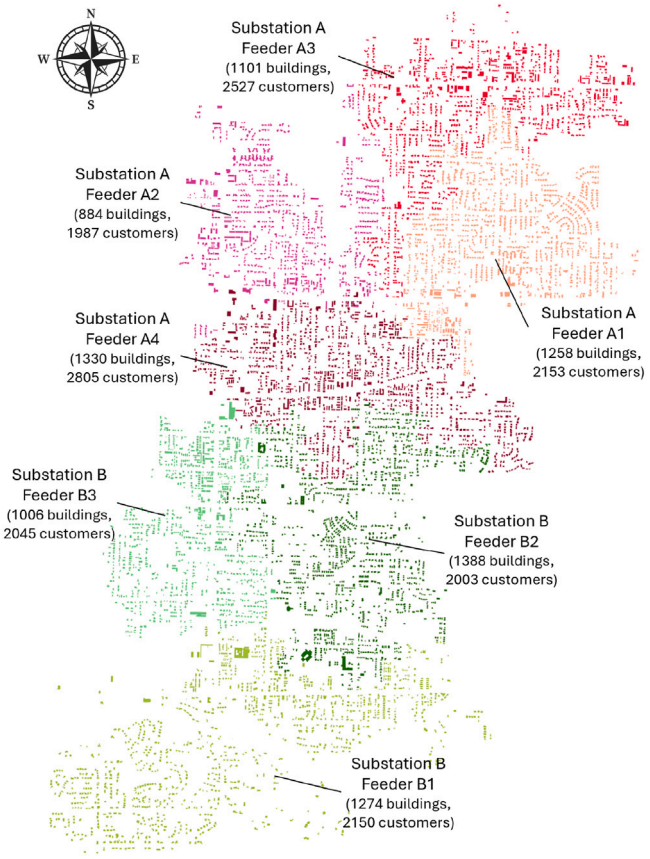

Fig. 5. Buildings and feeders within each substation and feeder selected for study.

Table 1
Building distribution across feeders and substations.

Substation	Feeder	Number of occupied buildings	Number of buildings with AC	Curtailed energy during outage (kWh)
A	A1	821	655	154,360
	A2	538	415	184,045
	A3	661	531	169,905
	A4	832	629	221,869
B	B1	930	721	232,560
	B2	1037	779	188,959
	B3	744	542	136,321

the outage was set to occur at 10:00 am on that day when the outdoor temperature started to climb up, and last until the end of June 29. It was assumed that occupants in 80% of the buildings would open windows for free cooling when outdoor conditions were favorable, more specifically, when the outdoor air temperature was at least 2 °C lower than the indoor temperature. On the other hand, to prevent overcooling, natural ventilation was disabled when the outdoor temperature dropped below 20 °C. The remaining 20% of buildings were assumed not to utilize natural ventilation, due to various factors such as living habits, occupant unavailability, window operability issues, or air quality concerns.

The building models were calibrated against the 2021 AMI data to reduce the discrepancy in electricity load prediction, and validated with the 2023 AMI data. Specifically, the occupancy schedules were inferred from the AMI data by identifying consecutive days of low consumption, suggesting non-occupied periods for each home and improving the model accuracy [28]. The model calibration was achieved through the adjustment of key parameters such as internal loads, occupancy schedules, natural ventilation, and cooling use behavior. The results at the substation level show that the peak load estimation during the summer period achieves a coefficient of variation of root-mean-square error of 19.7% at the hourly resolution. In addition, the daily peak load prediction during the four-day heatwave exhibited an average error of 2.6%, with the maximum load being underestimated by 0.3%. The normalized mean bias error is within 5% [29]. For the heatwave in 2023, the validation results show that the peak load has a maximum load underestimation of 1.3% and a daily peak prediction MAPE of 2.0%. Buildings without air conditioners or those not occupied during the outage window were not included in the analysis, as power outages in these situations would not lead to increased heat exposure for occupants during a heatwave.

5.2. Scenarios under study and data assumptions

The results are organized as follows. Initially, an outage-induced overheating risk assessment is presented for a 34-hour-long power outage, considering different levels of aggregation for the evaluation of the metric introduced in Section 3.1. Data from Portland reported 2 hour power outages during the heat wave event in June 2021 [30], while outages during Public Safety Power Shutoffs ranged from 33 to 66 hours [31]. The choice of a 34-hour-long power outage represents a low probability event [32], selected with the sole purpose of evaluating the metric over the heat wave duration and allowing an overheating sensitivity comparison across feeders. Then, the application of the method proposed in Section 4 for scheduling rotating outages for the feeders of Substation A is presented. Finally, the comparison between the performance of the proposed method versus random outage rotations that can be applied by utilities is discussed. The considered cases are listed below:

- *Case 1*: the outage-induced overheating risk is evaluated by aggregating data at substation level. In this case, the overheating risk is evaluated by combining all the consumers connected to the substation feeders. This aggregation allows prioritization of substations for rotating outage selection.
- *Case 2*: the outage-induced overheating risk is evaluated by aggregating data at feeder level. In this case, the metric is evaluated by aggregating consumers of each of the substation feeders to identify feeders with higher heat resilience, which are better candidates to be prioritized for the rotating outage scheduling.
- *Case 3*: a static scenario for rotating outage scheduling where the utility is required to reduce the substation load by at least 20% throughout the rotation window.
- *Case 4*: a static scenario where the utility is required to reduce the substation load by at least 40% throughout the rotation window.
- *Case 5*: a time-variant scenario where the utility is required to reduce 20% of the load during the first four hours, then 40% of the total load during the following four hours.
- *Case 6*: the performance of the proposed method is evaluated by comparing the resulting overheating risk and curtailed energy against randomly generated scenarios that represent uninformed utility action.

The rotation in cases 3–6 is evaluated over an 8-hour interval, with switching actions to be taken every hour. The outage-induced overheating risk curves that relate outage-induced overheating risk and outage duration for an outage starting at hour 10 are shown in Fig. 6. In addition, the maximum disconnection time for each feeder $\overline{d_f}$ of two hours and a minimum connected time $\underline{c_f}$ before disconnection of one hour are considered for the rotating outage scheduling.

It is worth pointing out that these curves show a growing trend that saturates after 8 hours have elapsed. This is due to this power outage starts at 10 am, and then after 8 hours, the outdoor air temperature starts reducing also lowering the overheating risk. The threshold for the metric calculation is assumed to be 90 °F (32.2 °C).

5.3. Case 1: Substation results for a long duration power outage

The metric's ability to identify the most sensitive substations to outage-induced overheating risk is evaluated considering an extreme condition of a 34-hour power outage. The study is applied to substations A and B, which have 4 and 3 feeders, respectively. The outage-induced overheating risk of each of the substations is summarized in Table 2. The metric is evaluated considering the accumulated overheating and energy curtailed for the complete set of buildings supplied by the substation.

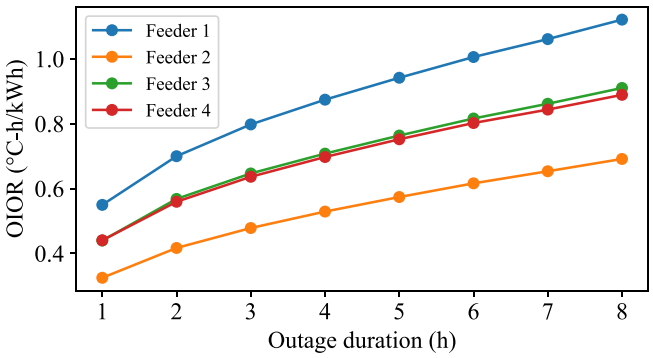

Fig. 6. Outage-induced overheating risk as a function of the outage duration for substation a feeders for an outage starting at 10 am.

Table 2
Aggregated Outage-Induced overheating risk at each substation.

Substation	Outage-Induced Overheating Risk (°C – h/kWh)
A	1.063
B	1.142

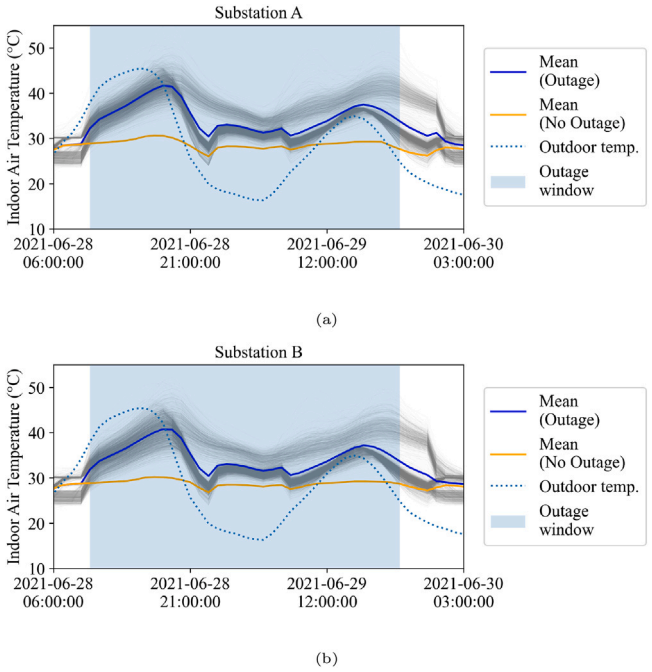

Fig. 7. Building indoor air temperature trajectories and averages during the 34-hour power outage: (a) substation A, and (b) substation B. Trajectories in gray correspond to indoor air temperature during outage only. Outdoor temperature is shown for reference.

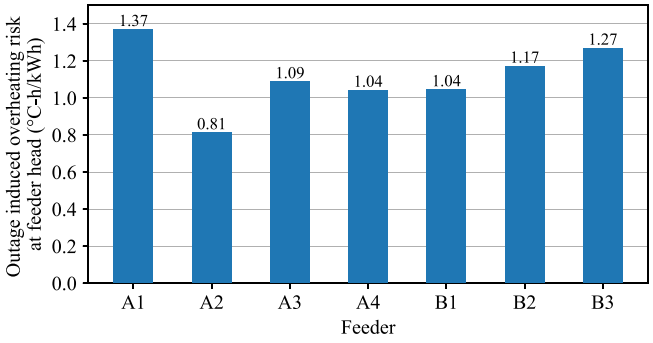

Fig. 8. Outage-induced overheating risk aggregated at each feeder head for all feeders in substations A and B.

When compared at a substation level, Substation B is slightly more sensitive to the power disconnection compared to substation A, as shown in Table 2. Substation B supplies a smaller set of buildings with AC compared to Substation A (2,230 buildings in substation A vs. 2,042 in substation B); hence, a lower energy consumption during the outage window compared to substation B leads to a higher sensitivity to the power outage. A comparison of temperature trajectories and average temperatures between buildings in Substation A and B is presented in Fig. 7. From Fig. 7, the average trajectories show the divergence of temperature values during the outage window, compared to the scenario with no outage. Comparing the average values across both feeders, the maximum average temperature is 41.6 °C (106.9 °F) for substation A while this value reaches 40.6 °C (105.1 °F) for substation B. Despite the higher peak in the hourly average temperature across buildings in Substation A, the intensity of overheating risk per kWh of energy curtailed leads to a greater impact on a smaller group of buildings. On identifying candidate substations, the application of the metric helps recognize substations with better capacity to withstand the negative effect of the power outage.

5.4. Case 2: feeder-level results for a long duration power outage

The results of the metric when buildings are aggregated at a feeder level are shown in Fig. 8, calculated considering the overheating risk and energy curtailed per feeder. This evaluates the direct impact of a feeder disconnection by the utility at the substation on the overheating risk experienced by consumers in the feeder. As for Substation A, Feeder A2 is the feeder with the lowest sensitivity to the power outage compared to the other feeders, followed by Feeder A4 and Feeder A3, with Feeder A1 being the most sensitive. In a rotating outage scenario, Feeder A2 is the most suitable candidate to start a rotation, while the disconnection of Feeder A1 may lead to the highest overheating risk across all feeders. Similarly for Substation B, Feeder B3 corresponds to the feeder with the largest sensitivity to the power outage, making it a better candidate to remain connected for longer periods during the rotating outage calculation.

5.5. Case 3: single-feeder rotating outage scheduling for substation A

The rotating outage scheduling is evaluated in Substation A for the cases introduced in Section 5.2. The rotating outage schedule for Case 3 is shown in Fig. 9(a). At all times, the disconnection of a single feeder is enough to meet the load reduction target. In this case, Feeder A2 is prioritized for disconnection during hour 10 as it corresponds to the feeder with the least sensitivity to the power outage. The disconnection of Feeder A2 during hour 1 reduces the load to meet the utility target, as shown in Fig. 9(d). For hour 11, it is more favorable to have Feeder A2 disconnected for one more hour than attempting to disconnect any of the other feeders, as shown by the metric evolution in Fig. 9(g). As Feeder A2 has reached its maximum time out, the feeder is reconnected, enforcing an outages in Feeder A3 for hour 12 and subsequently Feeder A4 during hour 13. Feeder A1 is considered as the final choice for the rotation due to its highest OIOR to the power outage in hour 14. Feeder A1 is reconnected in hour 15. At this hour, a complete rotation is obtained, leading Feeder A2 to become available for a new rotation and the rotation pattern from the initial hours is repeated starting hour 15.

5.6. Case 4: double-feeder rotating outage scheduling for substation A

The rotating outage schedule for Case 4 is shown in Fig. 9(b). To meet the load reduction target throughout the rotation, at least two feeders need to be disconnected each hour. Feeders A2 and A3 are prioritized for disconnection during hour 10. Similar to Case 1, Feeder A2 can be disconnected in two-hour intervals. Feeder A3 can only be disconnected for one hour before the overheating increases, switching with Feeder A4 during hour 11. In hour 12, Feeder A2 is reconnected after meeting the maximum disconnection time, and Feeder A4 is reconnected due to it is more favorable to disconnect Feeder A1 than to extend the disconnection time of Feeder A4. At this time, Feeders 2 to 4 are unavailable for disconnection. Since disconnection of Feeder 1 is not enough to meet the load reduction target, and no other candidate is available, Feeder A3 is removed from the locked list to be disconnected and meet the load reduction target, as seen in Fig. 9(e). This does not apply to Feeders A2 and A4 which must remain reconnected during hour 12, as the minimum on-time after reconnection has not been met. Feeder A2 can be disconnected again after meeting the minimum on-time after reconnection and can be disconnected for the next two hours, with Feeders A4 and A3 alternating during hours 13 and 14, with a reset at hour 14. The rotation pattern is repeated starting at hour 16.

5.7. Case 5: rotating outage scheduling for substation A under time-variable load reduction

The rotation for Case 5 is shown in Fig. 9(c). The scheduling replicates the rotation of Case 3 during the first four hours, where the required load reduction by the utility can be met by disconnecting a single feeder per hour. Starting hour 14, two feeder disconnections are required to meet the load reduction target. Feeder 4 is not available as

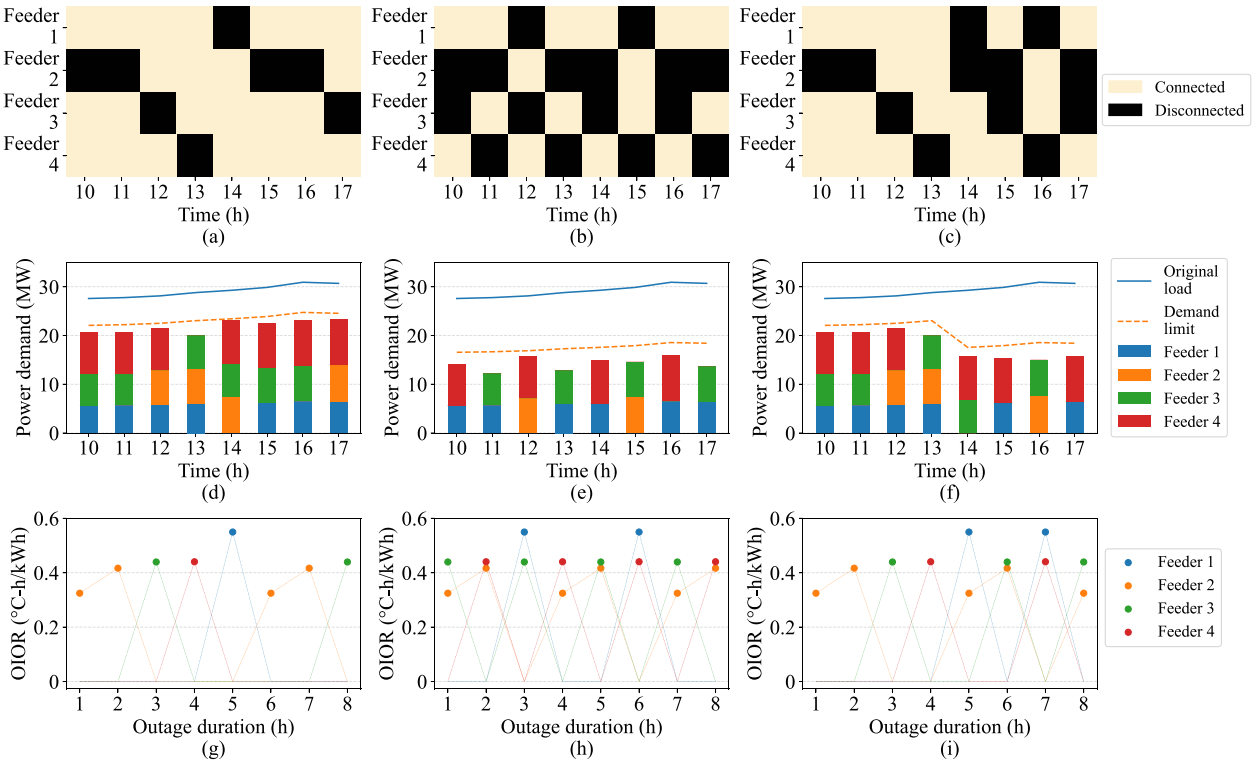

Fig. 9. Rotating outage schedules, energy curtailment, and outage-induced overheating risk metric for the considered cases. First row includes the rotating outage schedules. Second row includes the energy consumed by each feeder and load reduction target. Third row includes the value of the outage-induced overheating risk metric. Each column corresponds respectively to Case 3, Case 4, and Case 5.

a reconnection is enforced for hour 14, and Feeders A2 and A3 are in the locked feeder list. Then, a reset of the candidate feeders for disconnection is required removing Feeders A2 and A3 from the locked feeder list. With Feeder A2 as the available feeder with the lowest sensitivity, its disconnection combined with Feeder A1 allows meeting the load reduction target for the substation. For hour 15, feeder A1—which has the largest sensitivity—is reconnected and switched with feeder A3. A new reset is applied at hour 16 to enable feeder A1 and then the process is finalized with the disconnection of Feeders A2 and A3.

To assess the effect of variable outage conditions, a comparison of the cumulative overheating risk and energy curtailed for case 3 (one disconnection per hour), case 4 (two disconnections per hour), and case 5 over the rotating outage window is shown in Fig. 10. During the first four hours of the rotating outage, cases 3 and 5 follow the same overheating risk and curtailed energy trajectories, as both require a single feeder disconnection per hour. As the utility is required to curtail more load starting in hour 5, which implies disconnecting two feeders, both overheating risk and curtailed energy exhibit a steeper increase. From this hour onward, case 5 increases at nearly the same rate as Case 4, showing how tightened operational constraints reduce scheduling flexibility, leading to higher aggregated thermal stress for buildings supplied by Substation A.

5.8. Comparison against random strategies

To evaluate the quality of the obtained solution, 2,000 random rotating-outage schedules with two feeder disconnections per hour are generated, consistent with the load reduction requirement of Case 4. These scenarios emulate random actions at the substation to meet the load reduction target. For each of these Case-4 schedules, two additional schedules are derived from the same realization to represent Case 3 (one-feeder disconnection per hour) and Case 5 (mixed disconnection pattern). The combination of these three cases constitutes a triad of related schedules, which are required to satisfy the rotating outage constraints.

Out of 2,000 random realizations, 169 feasible triads are obtained. For each triad, the total outage-induced overheating risk is calculated as the sum of the overheating across all disconnection cases and then averaged across the three schedules. The average curtailed energy is also obtained. This aggregation provides a consistent performance comparison across operating conditions. The resulting objective space plot is shown in Fig. 11, which shows that, while the method is not conceived to be Pareto-optimal, the solution leads to the lowest average outage-induced overheating risk while maintaining moderate energy curtailment.

It is worth mentioning that sampling-based searches can become more complex when a large number of feeders or hours are considered, and the probability of drawing near-optimal solutions decreases with the problem size. In addition, emergency operations require fast response from distribution system operators. Sampling produces a set of Pareto optimal alternatives, increasing the decision load as operators must evaluate tradeoffs across multiple feasible solutions. By contrast, our method provides a single, high-quality schedule, reducing the decision-making burden during the emergency.

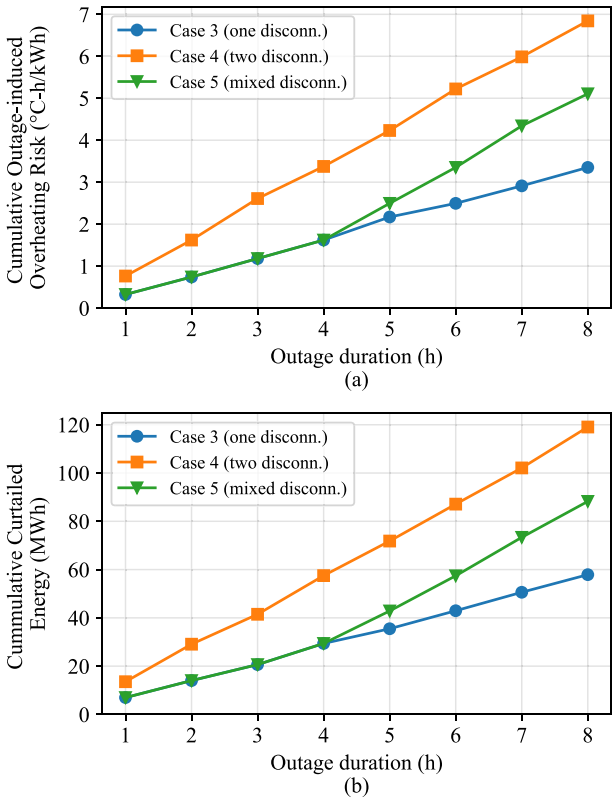

Fig. 10. Performance comparison between cases 3 to 5 over the rotating outage window: (a) cumulative overheating risk, and (b) cumulative energy curtailed.

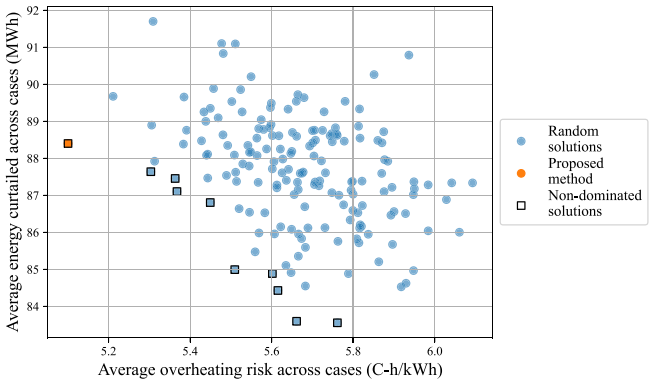

Fig. 11. Objective space plot for the random solution and the solution obtained using the proposed method.

6. Conclusion

6.1. Concluding remarks

This paper presents a framework for scheduling rotating outages based on indoor overheating risk, particularly during extreme heat events. Our approach introduces a quantitative metric that captures the additional overheating risk associated with power outages, enabling utilities to prioritize outage rotations that reduce the adverse effects of heat exposure on communities. By simulating the indoor air temperature during extreme heat events, combined with the electricity curtailed during the power outage, utilities can effectively identify the feeders in their territory that would experience the highest outage-related thermal stress.

The proposed methodology provides an efficient mechanism for power utilities to make rapid and informed decisions when rotating power outages are required, guided by community resilience to extreme heat events. The method provides flexibility by considering evolving conditions during the rotating outage window, such as changing load shedding requirements, and maximum disconnection periods for critical feeders. This represents an advantage as feeders with higher outage-induced overheating risk can be disconnected less frequently, reducing the heat exposure of more sensitive consumers.

From a utility regulatory and policy perspective, these results highlight the importance of incorporating heat vulnerability into rotating outage practices, moving from decisions based on load only to risk-informed strategies. In contrast to random and uninformed disconnections, which can unintentionally aggravate the effects of the heat wave on a community, the proposed method provides a mechanism that can be integrated into operations planning or regulatory guidance for outage management during extreme weather. Thus, power utilities can meet the power system reliability requirements while taking steps towards more resilient outage management strategies in times of increasing heat events.

6.2. Limitations and future work

The overheating risk calculation is based solely on indoor temperatures exceeding predefined thresholds, without accounting for the specific vulnerability of the building occupants. Certain groups, such as children, older adults, and people with pre-existing health conditions can be more sensitive to heat-related illness. In addition, we assume that customers do not take precautionary actions before the power outage, such as pre-cooling their homes. These limitations pave the way for future work. Further research should assess the impact of customer preparation on the scheduling of rotating outages. For instance, utilities could notify customers of potential power outages and incentivize pre-cooling strategies to reduce the risk of overheating. The information provided by this framework allows the identification of feeders where customers exhibit a lower thermal resilience after power outages, enabling power utilities to prioritize strategies towards risk mitigation in vulnerable communities, such as integrating distributed energy resources for additional power supply, or establishing resilience hubs to provide cooling during outages. Future work may also consider the potential of disconnecting sections of a feeder instead of a complete feeder disconnection. In this scenario, available reclosers throughout a feeder can add granularity to avoid disconnection of neighborhoods with larger overheating risks.

CRediT authorship contribution statement

Luis Rodriguez-Garcia: Writing – review & editing, Writing – original draft, Visualization, Validation, Software, Methodology, Formal analysis, Conceptualization. **Miguel Heleno:** Writing – review & editing, Supervision, Resources, Project administration, Methodology, Funding acquisition, Conceptualization. **Wanni Zhang:** Writing – original draft, Validation, Software, Data curation. **Han Li:** Writing – review & editing, Formal analysis. **Kaiyu Sun:** Writing – review & editing, Validation, Methodology, Data curation. **Tianzhen Hong:** Writing – review & editing, Project administration, Funding acquisition, Conceptualization.

Declaration of competing interest

The authors declare that they have no known competing financial interests or personal relationships that could have appeared to influence the work reported in this paper.

Acknowledgements

This research was supported by the Office of Electricity of the United States Department of Energy, under Contract No. DE-AC02-05CH11231. Any opinions, findings, and conclusions or recommendations expressed in this material are those of the author(s) and do not necessarily reflect

the views of the Department of Energy. Authors appreciate strong support from the team at Portland General Electric.

Data availability

The authors do not have permission to share data.

References

[1] Howard JT, Androne N, Alcover KC, Santos-Lozada AR. Trends of heat-related deaths in the US, 1999-2023. JAMA Oct 2024;332(14):1203–4. [Online]. Available: https://doi.org/10.1001/jama.2024.16386

[2] Ke X, Wu D, Rice J, Kintner-Meyer M, Lu N. Quantifying impacts of heat waves on power grid operation. Appl Energy 2016;183:504–12. [Online]. Available: https://www.sciencedirect.com/science/article/pii/S0306261916312971.

[3] Reeves J, Foelz C, Grace P, Best P, Marcussen T, Mushtaq S, Stone R, Loughnan M, McEvoy D, Ahmed I, Mullett J, Haynes K, Bird D, Coates L, Ling M. Impacts and adaptation response of infrastructure and communities to heatwaves: the southern Australian experience of 2009. Gold Coast, Queensland: National Climate Change Adaptation Research Facility. Dec 2010.

[4] California Independent System Operator. Emergency notifications fact sheet Aug, 2023, commPR/08.2023. [Online]. Available: https://www.caiso.com/documents/emergency-notifications-fact-sheet.pdf.

[5] Causes of California outages in 2020 and a remedy: geothermal power, 2021, presented at the IAEE Energy Forum, 2nd Quarter 2021. Available online: https://vhcenergy.com/vhc/wp-content/uploads/2022/01/IAEE-EnergyForum-2ndQ2021-CausesofCaliforniaOutagesin2020andARemedy-GeothermalPower.pdf [Accessed: 4 April 2025].

[6] Western Electricity Coordinating Council. Reliability and security dashboard — all indicators 2022 q3 (final). Report, Western Electricity Coordinating Council; February 9 2023. [Online]. Available: https://www.wecc.org/sites/default/files/documents/program/2024/Dashboard-All-Indicators%202022%20Q3%20%28Final%29.pdf.

[7] Pacific Gas and Electric Company (PG&E). Rotating outages, 2025,. [Online]. Available: https://www.pge.com/en/outages-and-safety/outage-preparedness-and-support/understanding-electric-outages/rotating-outages.html [accessed: 30 April 2025].

[8] Public Service Company of New Mexico (PNM). Protect the grid: strategic rotating outages, 2025,. [Online]. Available: https://www.pnm.com/protectthegrid [accessed: 30 April 2025].

[9] Shalaby AA, Abdeltawab H, Mohamed YA-RI. Towards resilient self-proactive distribution grids against wildfires: a dual rolling horizon-based framework. IEEE Trans Power Syst 2024:1–15.

[10] Hong T, Malik J, Krelling A, O'Brien W, Sun K, Lamberts R, Wei M. Ten questions concerning thermal resilience of buildings and occupants for climate adaptation. Build Environ 2023;244:110806. [Online]. Available: https://www.sciencedirect.com/science/article/pii/S0360132323008338.

[11] Rajput M, Augenbroe G, Stone B, Georgescu M, Broadbent A, Krayenhoff S, Mallen E. Heat exposure during a power outage: a simulation study of residences across the metro Phoenix area. Energy Build 2022;259:111605. [Online]. Available: https://www.sciencedirect.com/science/article/pii/S0378778821008896.

[12] Sun K, Zhang W, Zeng Z, Levinson R, Wei M, Hong T. Passive cooling designs to improve heat resilience of homes in underserved and vulnerable communities. Energy Build 2021;252:111383. [Online]. Available: https://www.sciencedirect.com/science/article/pii/S0378778821006678.

[13] Sheng M, Reiner M, Sun K, Hong T. Assessing thermal resilience of an assisted living facility during heat waves and cold snaps with power outages. Build Environ 2023;230:110001. [Online]. Available: https://www.sciencedirect.com/science/article/pii/S0360132323000288.

[14] Poudel S, Yu MG, Mukherjee M, Hanif S, Hardy TD, Reeve HM. A framework to design consumer-centric operational strategies for resilience enhancement. IEEE Trans Ind Appl 2024;60(2):2332–43.

[15] Bajagain S, Poudel S, Yu MG, Mukherjee M. Data-driven outage management scheme for enabling resilience during extreme events. In: 2025 IEEE PES grid edge technologies conference & exposition (grid edge); 2025. p. 1–5.

[16] Sun H, Kitamura S, Nikovski D. Fair blackout rotation for distribution systems under extreme weather events. In: 2022 IEEE PES innovative smart grid technologies conference Europe (ISGT-europe); 2022. p. 1–6.

[17] Rocha C, Green J, Holsomback V, Deaver B. Strategic load shedding for reduced impact of extreme weather events on distribution systems. In: CIRED Chicago workshop 2024: resilience of electric distribution systems, vol. 2024. 2025. p. 428–32.

[18] Agarwal A, Khandeparkar K. Distributing power limits: mitigating blackout through brownout. Sustain Energy Grids Netw 2021;26:100451. [Online]. Available: https://www.sciencedirect.com/science/article/pii/S2352467721000229.

[19] Raj BD, Kumar S, Padhi S, Sarkar A, Mondal A, Ramamritham K. Brownout based blackout avoidance strategies in smart grids. IEEE Trans Sustain Comput 2021;6(4):586–98.

[20] Raj BD, Sarkar A, Goswami D. An efficient framework for brownout based appliance scheduling in microgrids. Sustain Cities Soc 2022;83:103936. [Online]. Available: https://www.sciencedirect.com/science/article/pii/S221067072200258X.

[21] Wang Z, Hong T, Li H. Informing the planning of rotating power outages in heat waves through data analytics of connected smart thermostats for residential buildings. Environ Res Lett Jun 2021;16(7):074003. [Online]. Available: https://dx.doi.org/10.1088/1748-9326/ac092f.

[22] Rodriguez-Garcia L, Heleno M, Parvania M. Power distribution system planning for mitigating overheating risk inequity. IEEE Trans Power Syst 2025;40(1):920–32.

[23] Rodriguez-Garcia L, Heleno M, Parvania M. Assessing the impacts of power outage on community overheating risk during extreme heatwaves. In: Proceedings of the Hawaii international conference on system sciences 2024 (HICSS-57); 2024. p. 3. [Online]. Available: https://aisel.aisnet.org/hicss-57/es/renewable_resources/3.

[24] Lawrence Berkeley National Laboratory. CityBES: city building energy saver, 2024, https://citybes.lbl.gov/ [accessed: 10 June 2024].

[25] City of Portland. GIS open data portal; n.d., [Online]. Available: https://gis-pdx.opendata.arcgis.com/[Accessed: 11 June 2024].

[26] Northwest Energy Efficiency Alliance. 2022 residential building stock assessment. Tech. Rep., Northwest Energy Efficiency Alliance; 2022, [Online]. Available: https://neea.org/wp-content/uploads/2025/03/2022-Residential-Building-Stock-Assessment.pdf [accessed: 11 June 2024].

[27] NASA Langley Research Center. NASA power data access viewer; n.d., [Online]. Available: https://power.larc.nasa.gov/[Accessed: 11 June 2024].

[28] Li H, Heleno M, Sun K, Zhang W, Garcia LR, Hong T. Deciphering city-level residential ami data: an unsupervised data mining framework and case study. Energy AI 2025;20:100484. [Online]. Available: https://www.sciencedirect.com/science/article/pii/S2666546825000163.

[29] Zhang W, Sun K, Li H, Rodriguez-Garcia L, Heleno M, Hong T. Calibration of urban building energy model using smart meter data for district peak load prediction. Appl Energy 2026;407:127348. [Online]. Available: https://www.sciencedirect.com/science/article/pii/S0306261925020781.

[30] Staff KATU. PGE reports power outages amid record-breaking heat. Updated June 28, 2021. June 27 2021. [Online]. Available: https://katu.com/news/local/thousands-of-pge-customers-without-power-amid-heatwave.

[31] Portland General Electric Company. 2022 public safety power shutoff (PSPS) annual report. Report, Portland General Electric Company; December 28 2022. [Online]. Available: https://assets.ctfassets.net/416ywc1laqmd/2ORY2Yct3bE0KrkVbYDXz1/a5ef8c140031e270cdae3cec2323af3c/2022-12-28_PGE_PSPS_Annual_Report_FINAL.pdf.

[32] Saki S, Sofia G, Kar B, et al. A multi-year analysis of the impact of heatwaves and compound weather events on power outages. Sci Rep 2025;15:30846. [Online]. Available: https://doi.org/10.1038/s41598-025-15065-x